Adv. Studies Theor. Phys., Vol. 4, 2010, no. 8, 369 - 381

Surface Effect and Size Dependence on the Energy Release due to a Nano InAs Inclusion Expansion in a GaAs Matrix Material

Tong Hui and Yi-Heng Chen*

School of Aerospace, SVL, Xi'an Jiaotong University, 710049, P.R. China
*email: yhchen2@mail.xjtu.edu.cn

Abstract. This paper deals with the surface effect and size dependence on the energy release due to a nano InAs inclusion expansion in a plane GaAs matrix under uni-axial or bi-axial loadings. It is concluded that the surface effect inhibits the *M*-integral significantly and the *M*-integral may be either positive corresponding to the energy release or negative corresponding to the energy absorbing. This is because the mutual interaction between the external loading and the surface effect yields an additional contribution to the *M*-integral, which is always negative and proportional to the external loading.

Keywords: Nano-inclusion; M-integral; surface effect; mutual effect

1. Introduction

Nanotechnology involves analysis, design, and fabrication of devices and structures with at least one of the overall dimensions in the nanometer range. In recent years, quantum dot and wire structures have attracted considerable attention due to their potential application in nanotechnology[1-20]. This is because the mechanical and optoelectronic properties of nanocomposites are significantly influenced by the elastic field of the inhomogeneity. Thus, the elastic field of a nanoscale inhomogeneity in a matrix material has been well addressed by a number of researchers. For example, Tain and Rajapakse [14] obtained an analytical solution for the nano void or inclusion problems, from which the hoop stress along the void/inclusion as influenced by the surface parameters was well discussed.

2. The M-integral and energy release rate

In this paper, unlike the previous studies[1-20], attention will be focused on another topic: the energy release due to a nano InAs inclusion expansion in a plane GaAs matrix material as represented by the *M*-integral (see Fig. 1), which was classical used in macro elasticity[21-23]:

$$M = \oint_C (w x_i e_i - T_k u_{k,i} x_i) ds \ , \tag{1}$$

where *C* is a counterclockwise contour enclosed the whole nanosized inclusion as shown in Fig. 1, $w=\sigma_{ij}\varepsilon_{ij}/2$ denotes the strain energy density; and T_k is the traction acting on the outside of a closed contour *C*, x_j with j=1, 2 represents a rectangular plane coordinate system, e_i refers to the outside normal component of the contour *C* and *s* is the arc length of the contour *C*.

Because the *M*-integral is a global parameter while the surface tension and the surface Lamė constants are local parameters, physically, it is worth studying how the local parameters influence the global parameter, e.g., increase it or decrease it?

By using the Gurtin and Murdoch's model[24,25] that accounts for the surface tension and the surface Lamė constants, the *M*-integral for the InAs inclusion in a plane GaAs matrix material could be formulated as follows

$$M = \frac{\pi R(1+\kappa)\left[2\mathrm{Co1}(\sigma_{xx}^{\infty} - \sigma_{yy}^{\infty}) - \mathrm{Co2}(\sigma_{xx}^{\infty} + \sigma_{yy}^{\infty})\right]}{4\mu}, \tag{2}$$

where R is the radius of the inclusion, σ_{xx}^{∞} and σ_{yy}^{∞} are the applied loadings at infinity, κ and μ are elastic constants of the matrix GaAs, and

$$\begin{aligned} \mathrm{Co1} &= \frac{2}{\kappa+1}\left[-(\mu_1 - \mu + \eta_1^{(1)})A_{-11} + 3\eta_1^{(2)}A_{31}\right], \\ \mathrm{Co2} &= \frac{1}{\kappa+1}\left\{4\left[\left(\mu_1\frac{\kappa-1}{\kappa_1-1} - \mu + (\kappa-1)\eta_1\right)A_{11} + \frac{\kappa-1}{4}\sigma_0\right]\right\}. \end{aligned} \tag{3}$$

with $\eta_1 = (2\mu_0 + \lambda_0)/(4R)$, $\eta_1^{(1)} = \eta_1 + 0.25\sigma_0/R$, $\eta_1^{(2)} = \eta_1 - 0.25\sigma_0/R$, λ_1 and μ_1 are elastic constants of the inclusion InAs, σ_0, μ_0 and λ_0 are the surface tension and the two surface Lamė constants along the interface between InAs and GaAs bi-material, respectively.

Note that the Lamé constants for InAs: λ_1=50.66 GPa, μ_1=19.0 GPa are much smaller than those for InAsλ=64.43 GPa, μ=32.9 GPa for GaAs [13,14]. Therefore, Fig. 1 shows a soft inclusion problem. As the surface Lamė constants μ_0 and λ_0 have some anisotropic feature in general[13,14] and they always appear together in the coefficient η_1 of Eq. (3), it is convenient to introduce a new parameter $K^S = \lambda_0 + 2\mu_0$ varying between -10N/m and 10N/m [14], whereas the surface tension σ_0 is assumed to be either zero or 0.72N/m for making comparison[13,14].

3. Numerical results and discussions

Numerical results for a 5nm InAs inclusion in the GaAs matrix material under a uni-axial tensile loading, a bi-axial tensile loading, and a bi-axial tensile-compression loading are plotted in Figs. 2(a,b,c), respectively. Here, the surface tension σ_0 is chosen to be 0.72N/m and the surface parameter K^S are chosen to be -10N/m, 0, and +10N/m, respectively. It is found from Fig. 2(a) that the black curve without any surface effect is far apart from the other three curves labeled by ■, thin curve and △, respectively, as the tensile loading varies from zero to 300MPa. Thus, the surface tension σ_0 influences the *M*-integral significantly, while the positive value of K^S slightly decreases the *M*-integral and the negative value of K^S slightly increases the *M*-integral, especially when the tensile loading is higher. This means that the parameter $K^S = \lambda_0 + 2\mu_0$ yields a small influence on the *M*-integral when the tensile loadings is relatively lower, say, $\sigma_{yy}^{\infty} < 100MPa$. However, the relative errors induced from the three values of K^S : -10, 0, and +10, become larger and larger when the tensile loading increases. The negative value of K^S always yields larger values of the *M*-integral as compared with those of K^S =0, while the positive value of K^S always yields smaller values of the integral. After comparing the black curve without any surface effect to the three curves with different kinds of the surface effect, it is concluded that the surface effect significantly inhibits the *M*-integral or the energy release due to the nano inclusion expansion under the tensile loading. Moreover, Fig.2(a) clearly reveals a significant physical phenomenon that, unlike those in classical defect mechanics without the surface effect, the *M*-integral could be either positive (as it would be in macro defect mechanics with a soft inclusion) or negative, depending on the tensile loading levels. For example, it is seen from Fig. 2(a) that as the tensile loading increases from zero, the *M*-integral decreases from zero either, showing a negative feature rather than a positive feature. This is contrary to the previous understanding on the energy release due to a soft inclusion expansion. This again clearly reveals that the expansion of the InAs inclusion under the tensile loading does absorb energy, rather than release energy. As the tensile loading increases monotonically, a neutral loading point reaches in Fig. 2(a), i.e., around 175MPa, at which a transformation of the *M*-integral from a negative value to a positive value occurs. Physically, this is an energy balance point, at which the expansion of the InAs inclusion in GaAs matrix could neither absorb nor release energy. Moreover, as the tensile loading increases monotonically further, the *M*-integral becomes positive and then the expansion of the InAs releases energy as it would be in classical macro defect mechanics.

Fig. 2(b) shows the numerical results of the *M*-integral against the bi-axial tensile loading with $\sigma_{yy}^{\infty} > 0$ and $\sigma_{xx}^{\infty} = \sigma_{yy}^{\infty}$. It is found that the black curve without any surface effect is far apart from the other three curves labeled by ■, thin curve and △ either. Moreover, the variable tendencies of the three curves are quite different from those under the uni-axial tensile loading shown in Fig.2(a). As both loadings σ_{xx}^{∞} and σ_{yy}^{∞} increase from zero simultaneously, the *M*-integral always decreases from zero showing negative values and representing the energy absorbing due to the expansion of the InAs inclusion in the GaAs matrix. It is concluded that the bi-axial tensile loading significantly increases the inhibiting effect of the surface effect on the *M*-integral.

Fig. 2(c) shows the numerical results of the *M*-integral against the bi-axial tensile compression loading with $\sigma_{yy}^{\infty} > 0$ and $\sigma_{xx}^{\infty} = -\sigma_{yy}^{\infty}$. It is found that variable tendencies are quite different from the above two cases shown in Figs.2(a,b). As the magnitudes of both the tensile loading and the compression loading increase from zero simultaneously, the *M*-integral always increases from zero showing positive values and representing the energy release induced from the expansion of the InAs inclusion in the GaAs matrix. It is concluded that the bi-axial tensile compression loading significantly decreases the inhibiting effect of the surface effect on the *M*-integral. From the physical point of view, different kinds of the external loadings may yield quite different results for the energy release or absorbing due to the expansion of the InAs inclusion as influenced by the surface effect.

The influence of inclusion radius on the *M* integral is plotted in Figs.3(a,b,c) under the three different kinds of external loadings. It is seen that as the radius decreases from 20nm to 1nm, the *M*-integral decreases very sharply under each of the three different kinds of the loadings. This again demonstrates that the surface effect inhibits the

M-integral. That is, the surface effect could change the physical feature from release energy to absorbing energy due to the expansion of the InAs inclusion in the matrix-inhomogeneity system.

It is very surprised that why so small surface parameters with an order of N/M (i.e., 10^{-10} less than the elastic moduli of InAs or GaAs) could influence the global parameter *M*-integral significantly?

From the physical point of view, a detailed explanation is needed. This can be done by dividing the *M*-integral into two distinct parts: $M = M^{(1)} + M^{(1,2)}$ which represent the contribution induced merely from the external loading and the contribution induced from the mutual effect between the external loading and the surface parameters $\sigma_0 = 0.72N/m$ and K^S = -10, 0, +10N/m, respectively. As plotted in Figs. 4(a,b), 5(a,b) and 6(a,b) under the three different kinds of loadings, respectively, it is seen that the first part, $M^{(1)}$, always shows a quadratic feature with respect to the external loading σ_{yy}^{∞} (see the curves with ● or ○), while the second part, $M^{(1,2)}$, always shows a negative and proportional feature with respect to σ_{yy}^{∞} (see the curves with ▲and △. Therefore, whether the overall *M*-integral with ■ or □ is positive depends on the difference between the two parts: $M^{(1)}$ and $M^{(1,2)}$. It is concluded that the reason as why the surface effect inhibits the *M*-integral significantly is clearly because of the mutual interaction between the external loading and the surface effect, which yields an additional contribution to the *M*-integral, $M^{(1,2)}$, which is always negative and proportional to the external loading.

References

[1] T. Kuzumake, K. Miyazawa, H. Ichinose, and K. Ito, Processing of carbon nanotube reinforced aluminum composite, J. Mater. Res., 13 (1998), 2445-2449.

[2] Y.Cui, and C. M. Lieber, Functional Nanoscale Electronic Devices Assembled Using Silicon Nanowire Building Bloks , Science, 291(2001), 851-853.

[3] E.W. Wong, P. E. Sheehan, and C.M. Lieber, Nanobeam Mechanics: Elasticity, Strength, and Toughness of Nanorods and Nanotubes, Science, 277(1997), 1971-1975.

[4] S. Cuenot, C. Frétigny, S. Demoustier-Champagne, and B. Nysten, Surface

tension effect on the mechanical properties of nanomaterials measured by atomic force microscopy, Phys.Rev. B, 69(2004), 165410.

[5] R.C. Cammarata, Surface and interface stress effects on interfacial and nanostructured materials, Mater. Sci. Eng., A, 237(1997), 180-184.

[6] R.E. Miller, and V.B. Shenoy, Size-dependent elastic properties of nanosized structural elements, Nanotechnology, 11(2000), 139-147.

[7] P. Sharma, S. Ganti, and N. Bhate, Effect of surfaces on the size-dependent elastic state of nano-inhomogeneities, Appl. Phys. Lett., 82 (2003), 535-537.

[8] P. Sharma, and S. Ganti, Size-Dependent Eshelby's Tensor for Embedded Nano-Inclusions Incorporating Surface/Interface Energies, ASME J. Appl. Mech., 71 (2004), 663-671.

[9] H.L. Duan, J. Wang, Z.P. Huang, and B.L. Karihaloo, Size-dependent effective elastic constants of solids containing nano-inhomogeneities with interface stress, J. Mech. Phys. Solids, 53(2005),1574-1596.

[10] V.B. Shenoy, Atomistic calculations of elastic properties of metallic fcc crystal surfaces, Phys. Rev. B, 71(2005), 094104.

[11] F. Yang, Size-dependent effective modulus of elastic composite materials: Spherical nanocavities at dilute concentrations, J. Appl. Phys., 95(2004), 3516-3520.

[12] H.L. Duan, J. Wang, Z.P. Huang, and Z.Y. Luo, Stress concentration tensors of inhomogeneities with interface effects, Mech. Mater., 37(2005), 723-736.

[13] P. Sharma, and S. Ganti, Interfacial Elasticity Corrections to Size-Dependent Strain-State of Embedded Quantum Dots, Phys. Status Solidi B, 234(2002), R10-R12.

[14] L. Tian, and R. K. N. D. Rajapakse, Analytical Solution for Size-Dependent Elastic Field of a Nanoscale Circular Inhomogeneity, ASME J. Appl. Mech., 74 (2008), 568-574.

[15] H.S. Park, and P.A. Klein, Surface stress effects on the resonant properties of metal nanowires: The importance of finite deformation kinematics and the impact of the residual surface stress, J. Mech. Phys. Solids., 56(2008), 3144-3166.

[16] S.G. Mogilevskaya, S.L. Crouch, and H.K. Stolarski, Multiple interacting circular nano-inhomogeneities with surface/interface effects , J. Mech. Phys. Solids, 56(2008), 2298-2327.

[17] C.W. Lim, Z.R. Li, and L.H. He, Size dependent, nonuniform elastic field inside a nano-scale spherical inclusion due to interface stress, Int. J. Solids Struct., 43(2006), 5055-5065.

[18] R. Dingreville, J. Qu, and M. Cherkauoi, Surface free energy and its effect on the elastic behavior of nano-sized particles, wires and films, J. Mech. Phys. Solids., 53(2005),1827-1854.

[19] J. Marian, J. Knap, and M. Ortiz, Nanovoid deformation in aluminum under simple shear, Acta Mater., 53(2005), 2893-2900.

[20] H.L. Duan, J. Wang, Z.P. Huang, and B.L. Karihaloo, Eshelby formalism for nano-inhomogeneities, Proc. R. Soc. London Ser. A, 461(2005), 3335-3353.

[21] J.K. Knowles, and E. Sternberg, On a class of conservation laws in linearized and finite elastostatics, Arch. Rat. Mech. Anal., 44 (1972), 187-211.

[22] B. Budiansky, and J.R. Rice, Conservation laws and energy-release rates, ASME J. Appl. Mech ,40(1973), 201.

[23] A.G. Herrmann, and G. Herrmann, On Energy-Release Rates for a Plane Crack, ASME J. Appl. Mech ,48(1981), 525-528.

[24] M.E. Gurtin, and A.I. Murdoch, A continuum theory of elastic material surfaces, Arch. Ration. Mech. Anal., 57(1975), 291-323.

[25] M.E. Gurtin, J. Weissmuller, and F. Larché, A general theory of curved deformable interfaces in solids at equilibrium , Philos. Mag. A, 78(1998), 1093-1109.

Figures Captions

FIG.1. A circular InAs nano-inclusion in a GaAs matrix material under bi-axial loadings.

FIG.2. The variable features of the *M* integral: (a) uni-axial tension loading, (b) bi-axial tension loading, (c) bi-axial tension-compression loading.

FIG. 3. The influence of inclusion radius on the *M* integral: (a) uni-axial tension loading, (b) bi-axial tension loading, (c) bi-axial tension-compression loading.

FIG.4. Values of M, $M^{(1)}$ and $M^{(1,2)}$ against the uni-axial tension loading: (a) with surface tension and positive surface modulus. (b) with surface tension and negative surface modulus.

FIG.5. Values of M, $M^{(1)}$ and $M^{(1,2)}$ against the bi-axial tension loading: (a) with surface tension and positive surface modulus. (b) with surface tension and negative surface modulus.

FIG. 6. Values of M, $M^{(1)}$ and $M^{(1,2)}$ against the bi-axial tension compression loading: (a) with surface tension and positive surface modulus. (b) with surface tension and negative surface modulus.

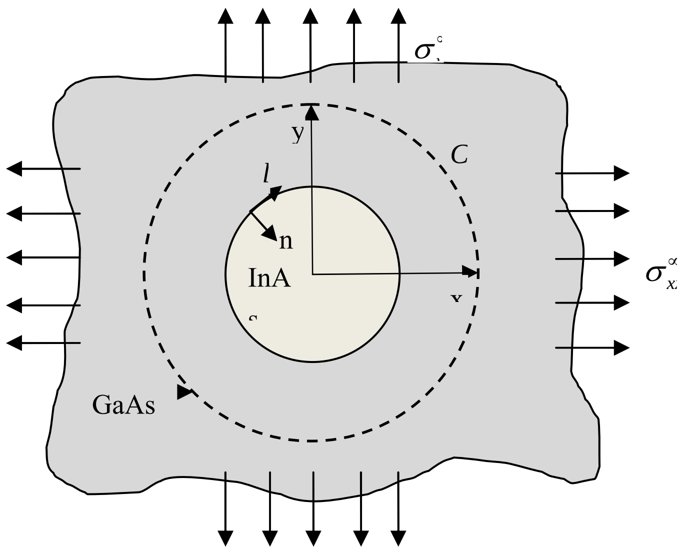

Fig. 1

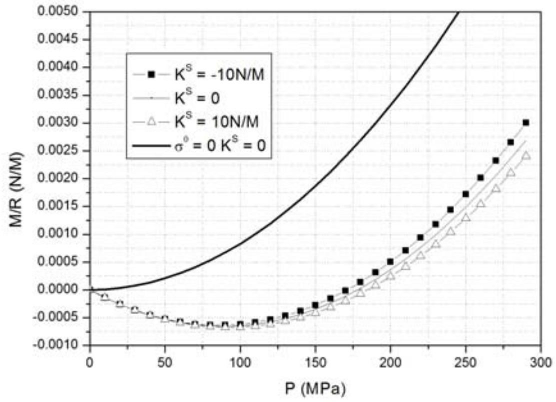

Fig. 2(a)

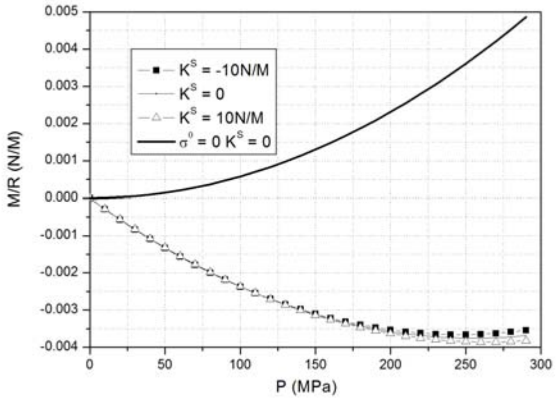

Fig.2(b)

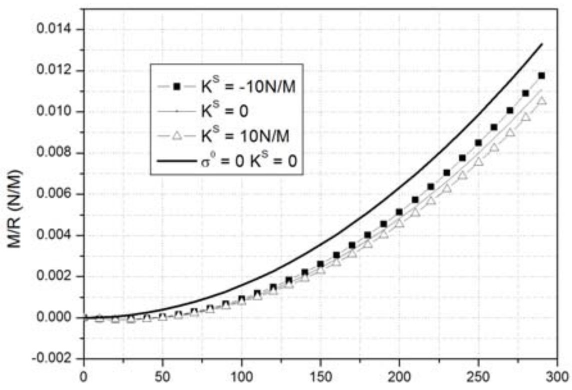

Fig.2(c)

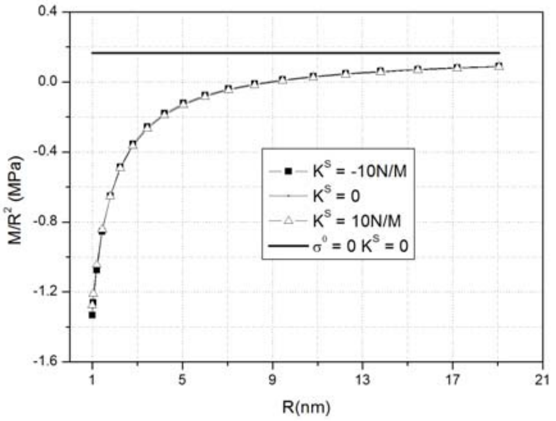

Fig.3(a)

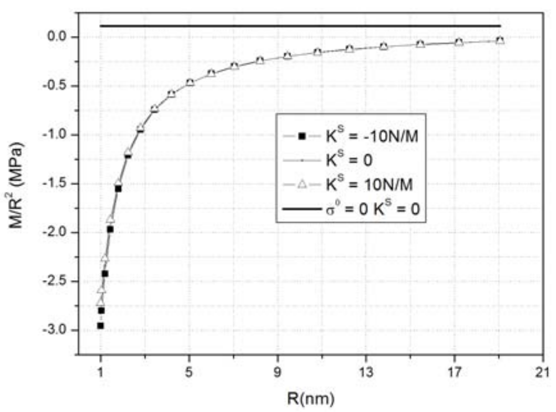

Fig.3(b)

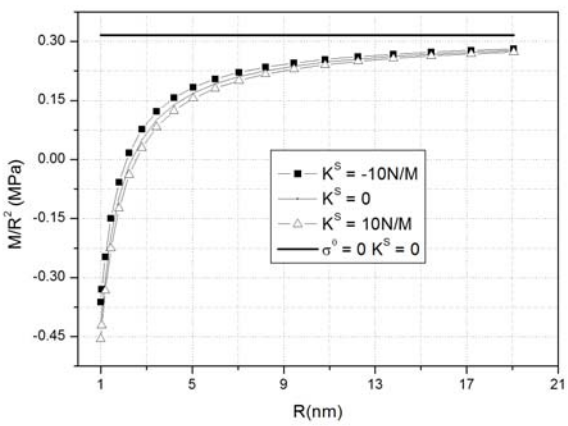

Fig.3(c)

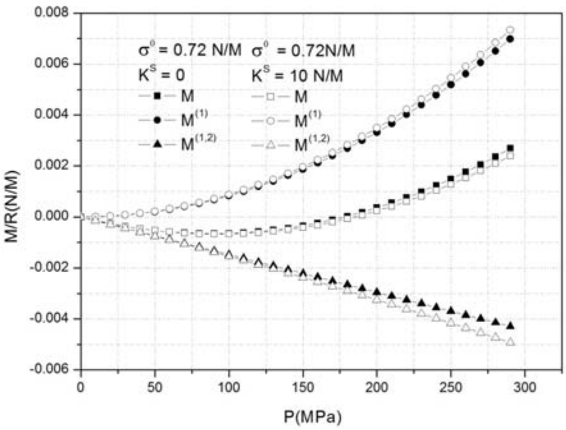
0.008
0.006
0.004
0.002
0.000
-0.002
-0.004
-0.006
0
50
100
150
200
250
300
M/R(N/M)
P(MPa)
σ⁰ = 0.72 N/M
K^S = 0
σ⁰ = 0.72N/M
K^S = 10 N/M
M
M(1)
M(1,2)

Fig.4(a)

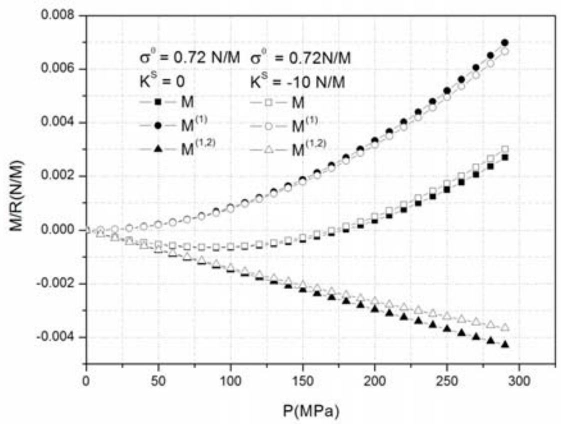
0.008
0.006
0.004
0.002
0.000
-0.002
-0.004
0
50
100
150
200
250
300
M/R(N/M)
P(MPa)
σ⁰ = 0.72 N/M
K^S = 0
σ⁰ = 0.72N/M
K^S = -10 N/M
M
M(1)
M(1,2)

Fig.4(b)

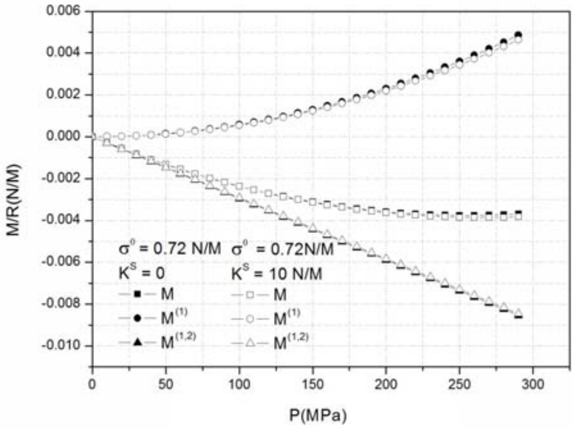
0.006
0.004
0.002
0.000
-0.002
-0.004
-0.006
-0.008
-0.010
M/R(N/M)
0
50
100
150
200
250
300
P(MPa)
σ° = 0.72 N/M
K^S = 0
M
M^(1)
M^(1,2)
σ° = 0.72N/M
K^S = 10 N/M
M
M^(1)
M^(1,2)

Fig.5(a)

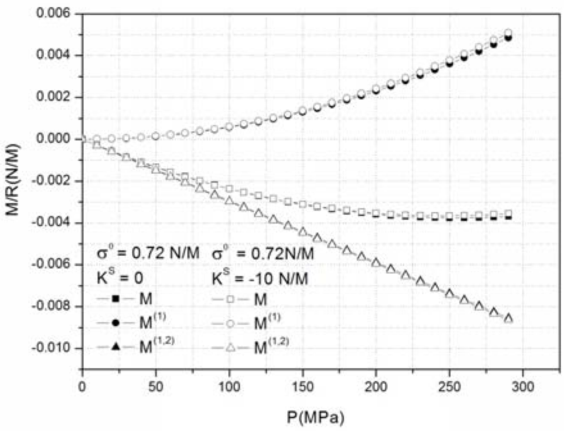
0.006
0.004
0.002
0.000
-0.002
-0.004
-0.006
-0.008
-0.010
M/R(N/M)
0
50
100
150
200
250
300
P(MPa)
σ° = 0.72 N/M
K^S = 0
M
M^(1)
M^(1,2)
σ° = 0.72N/M
K^S = -10 N/M
M
M^(1)
M^(1,2)

Fig.5(b)

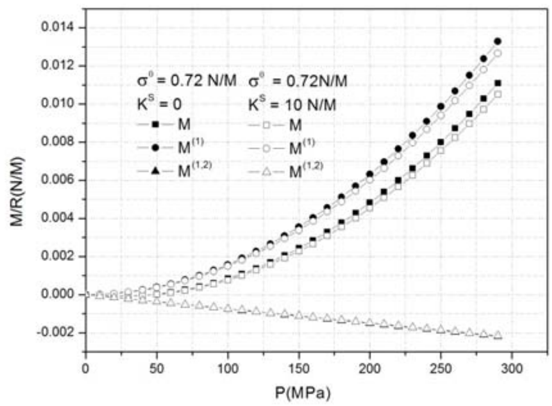

Fig.6(a)

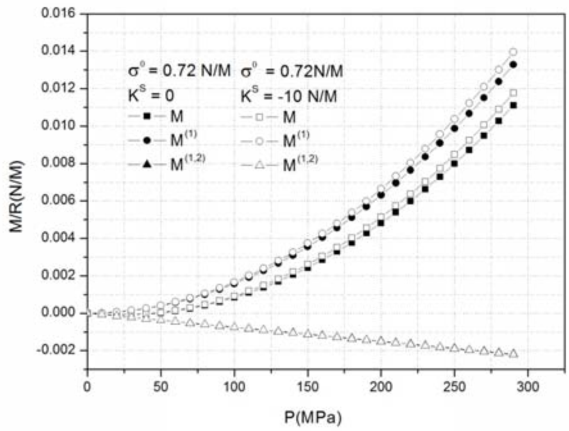

Fig.6(b)

Received: November, 2009